Heterogeneous expectations in the housing market: A Sugarscape agent-based model

Daehyeon Park[1] · Jengei Hong[2] · Doojin Ryu[1,*]

[1] Department of Economics, Sungkyunkwan University, Seoul, Korea
[2] School of Management and Economics, Handong Global University, Pohang, Gyeongsangbuk-do, Korea

*** Correspondence**:
Address: Department of Economics, Sungkyunkwan University, 25-2, Sungkyunkwan-ro, Jongno-gu, Seoul, Korea, 03063
E-mail: doojin.ryu@gmail.com

Abstract

This study examines the influence of heterogeneous expectations between buyers and sellers on housing market cycles. We propose an agent-based model that integrates houses into a Sugarscape model for analyzing housing market dynamics. Our model incorporates spatial factors into pricing by requiring agents to evaluate a property's value based on its location. Agents have limited information because they base their decision-making on spatial information. We investigate the impact of agents' visual range and the heterogeneity of their expectations regarding housing prices. Our simulations with different vision levels show that as agents expand their field of vision, the housing market experiences heightened buying competition, thereby increasing both average housing prices and market volatility. Simulation results with different heterogeneity levels show that when people have more homogeneous expectations, the housing market becomes more volatile. As heterogeneity decreases, the volatility of house prices increases more rapidly, implying that agents' homogeneous expectations reinforce feedback in the system, leading to higher volatility and more complex dynamics.

Keywords: Adaptive expectations; Agent-based model; Heterogeneity; Housing market; Sugarscape model

JEL Classifications: E32; E71; R31

1. Introduction

Housing-price cycles are complex and multifaceted phenomena influenced by various economic factors (Gomez-Gonzalez, Gamboa-Arbeláez, Hirs-Garzón, and Pinchao-Rosero, 2018; Park and Ryu, 2021). The rational expectations hypothesis suggests that external shocks cause housing price fluctuations because traders are assumed to directly observe the economy's current state. However, following the global financial crisis caused by the boom and bust in the housing market during 2000–2007, several studies have attempted to endogenously explain housing price fluctuations

(Geanakoplos, Axtell, Farmer, Howitt, Conlee, Goldstein, Hendrey, Palmer, and Yang, 2012). House traders' bounded rationality, which implies that they are rational, but the information they hold is restricted, is reflected in these models as an important factor that helps explain the endogenous cycle of housing-price dynamics (Burnside, Eichenbaum, and Rebelo, 2016). The role of imperfect rationality is particularly significant in housing markets because of the locations of houses. Housing assets occupy different locations, making the value of each property inherently unique and difficult to standardize. As a result, market participants cannot directly observe the fundamental value of each house (Duca, Muellbauer, and Murphy, 2021). In other words, the difficulty in observing the location values of houses hinders households' ability to capture the fundamental values of houses compared with other financial markets such as stock and bond markets.

This study investigates how the behavior of market participants under limited information about the value of a location generates housing cycles. Considering the locations of houses is essential for understanding why market participants do not always maintain rational expectations. The value of a house is determined by its location; however, the heterogeneity of houses, as each house is built on a unique site, makes it difficult for individual households to assess the value of a property independently. As mentioned by Shiller (2020), this complexity impedes the objective and independent calculation of housing value, leading market participants to form expectations in a more heuristic manner by relying heavily on observed prices, rumors, and news. Previous studies on bounded rationality and housing cycles have rarely considered the role of location, describing houses simply as identical durable goods or assets (Hong and Ryu, 2023). In this study, we explicitly consider the role of location heterogeneity to investigate the relationship between limited location information and house-price cyclicality.

We adopt an agent-based approach to analyze housing price fluctuations by considering the locations of houses. Individual agents are represented in an agent-based model (ABM) and their interactions are simulated to model the system's collective behavior (Park and Ryu, 2022, 2023). Each agent in the model is a basic unit in the system, with the ability to make decisions and act autonomously based on their internal state and environment. To mimic and simulate these interactions, the ABM uses a set of rules and algorithms ranging from simple decision-making processes to more complex ones that involve multiple agents adapting to a dynamic and changing environment. An ABM aims to understand the behavior of a complex system by representing it as a collection of interacting agents. A classic example of an ABM in sociology is the Sugarscape model developed by Epstein and Axtell (1996) to study the dynamics of societies and economies. The Sugarscape model represents a simple abstract world comprising a two-dimensional grid of cells, each with varying amounts of sugar. In this model, the term "sugar" is a metaphorical representation of an economic resource. Agents can move from cell to cell, harvesting sugar and consuming it. The agents in the Sugarscape model have simple rules governing their behavior. For example, they can choose to move to cells with higher levels of sugar or trade sugar with other agents. Additionally, agents have characteristics that can influence their behavior, such as age, health, and wealth. In the Sugarscape model, agents interact with each other and the environment to shape complex behavioral patterns such as market formation, emerging inequalities in wealth, and access to resources. Furthermore, the model demonstrates how social and economic systems evolve, with new patterns developing as agents adapt their behavior to the changing conditions.

The Sugarscape model explores the dynamics of social and economic systems and examines how complex behaviors arise from simple interactions between agents. This model is also an important example of how ABMs can be used to study complex systems in other fields such as economics and ecology. The Sugarscape model is appropriate for analyzing the housing market because it is based on spatial information. We create an ABM to analyze the housing market by adding houses in which agents reside into the Sugarscape model. In the proposed model, a house represents a location that provides access to its surroundings. This method captures two important features. First, a location's value is determined by how efficiently it provides access to other locations. In previous models, the value of a house is usually simplified as the utility derived from the house as a durable good. However, by explicitly considering the location of a house, we can more directly and rigorously analyze how the value of heterogeneous locations has evolved. Second, it recognizes the heterogeneity of houses because their locations are unique. Owing to the heterogeneity of these locations, each agent has only limited information on the expected values of houses. Housing prices, formed under limited information, fluctuate through the continuous exploration of location value and housing transactions. In turn, this generates cyclicality in overall housing prices.

We incorporate houses into the Sugarscape model by enabling agents to obtain economic resources by residing in their houses. In the model, the value of a house is determined by the potential gains generated from living there. Based on this value and the prevailing market rate, individuals trade houses. Our study investigates the impact of agents' vision and heterogeneous expectations on housing-price dynamics. Our simulation results reveal that as agents' field of vision widens, housing demand becomes more fiercely competitive, resulting in a notable increase in both average housing prices and market volatility. Furthermore, a greater degree of homogeneity in expectations among individuals contributes to heightened volatility in the housing market.

This study contributes to the existing research in several ways. First, it extends the suitability of the Sugarscape model to analyze the housing market by incorporating houses. Second, it reproduces housing-price cycles while considering the restricted spatial information of agents. Third, it investigates the impact of heterogeneity on investors' expectations of housing price volatility.

The remainder of this paper is organized as follows. Section 2 reviews the related literature. Section 3 presents the ABM for the housing market. Section 4 presents and discusses the results of the model simulation. Finally, Section 5 concludes the study.

2. Literature Review and Backgrounds

Housing-price dynamics have been the subject of extensive research, yielding several models and theories. Case and Shiller (1989) emphasize the difficulty of accurately forecasting individual housing price changes. Despite this challenge, they identify the presence of a profitable trading rule for those adept at timing their home purchases. This insight highlights the importance of timing in housing markets. Housing prices can temporarily deviate from their fundamental values, moving in the opposite direction of rational expectations (Clayton, 1996, 1997). Housing prices tend to move toward equilibrium prices, with two groups of factors determining price changes: factors explaining changes in equilibrium prices and those explaining deviations from the equilibrium (Abraham and Hendershott, 1996). The housing market's volatility can be influenced

by several factors, including supply elasticity, the business environment, and the role of monetary policy (Glindro, Subhanij, Szeto, and Zhu, 2011; McDonald and Stokes, 2013). However, small shocks can cause large fluctuations in asset prices because credit limits and asset prices are interrelated (Kiyotaki and Moore, 1997). Thus, understanding credit limits becomes crucial in housing market research. Iacoviello (2005) and Iacoviello and Neri (2010) expand on this by demonstrating how nominal debt can help stabilize an economy under interest rate control, particularly in mitigating supply shocks. Furthermore, they reveal that spillovers from the housing market can significantly affect consumption patterns. In contrast, Erlingsson, Teglio, Cincotti, Stefansson, Sturluson, and Raberto (2014) reveal that easy access to credit can increase housing prices, making the housing market more prone to recessions. (Lambertini, Mendicino, and Punzi, 2017) demonstrate that news shocks and incorrectly anticipated monetary policies can cause business cycle fluctuations, while credit frictions can cause boom-and-bust housing market cycles.

Several studies into the role of investor behavior in housing price dynamics reveal another layer of complexity. Burnside, Eichenbaum, and Rebelo (2016) propose that boom-and-bust episodes in housing markets may be driven by the interplay between skeptical and optimistic agents. In their model, agents have heterogeneous expectations and interact socially to persuade other agents. Meanwhile, Black, Fraser, and Hoesli (2006) and Damianov and Escobari (2016) suggest that housing-price dynamics are driven by momentum behavior. Capozza and Seguin (1996) find that the price-to-rent ratio can be an effective predictor of appreciation rates, but housing market participants may overreact to income growth. Cheng, Raina, and Xiong (2014) and Chinco and Mayer (2016) suggest that a lack of awareness of housing market issues can cause mispricing in the housing market. Granziera and Kozicki (2015) investigate whether irrational expectations can explain housing price fluctuations and the price-to-rent ratio in the United States. Piazzesi and Schneider (2009) discuss how optimists can raise transaction prices in the housing market.

Previous studies show that adaptive rational expectations can cause price fluctuations. The concept of adaptive rational expectations suggests that economic actors form subjective expectations based on their experiences (Brock and Hommes, 1997). These expectations interact with those of other agents to shape the economic environment collectively. Economic agents receive rewards based on their expectations and update them accordingly in response to new information. This creates an ecology of co-evolving expectations, which can only be analyzed through computations (Bolt, Demertzis, Diks, Hommes, and van der Leij, 2019). As households interpret observed house-price movements caused by changes in expectations as changes in fundamentals, price movements, and expectations amplify each other (Gelain and Lansing, 2014). Dieci and Westerhoff (2012, 2016) introduce a speculative housing market model in which agents use regressive forecasting rules to form their expectations. Their model dynamics exhibit irregular boom-and-bust cycles. Glaeser and Nathanson (2017) suggest that homebuyers' expectations lead to excess long-term volatility in house prices, which is consistent with prior survey evidence.

Our study employs an ABM to analyze how heterogeneous expectations affect housing prices. In an ABM, agents can autonomously decide their actions and interact within a simulated virtual space (Axtell, Axelrod, Epstein, and Cohen, 1996). This characteristic of an ABM makes it easy to incorporate individual heterogeneity into the model (Rahmandad and Sterman, 2008). When agents have limited information about the decisions of others, the complexity of their interactions makes it challenging to find equilibria in a mathematical model. However, an ABM

is well suited for simulations, including agent-based simulations. Such simulations involve constructing a complex ABM and using it to observe the specific behavioral patterns of agents.

ABMs are powerful tools for analyzing complex systems and have been used in several fields, including economics. An ABM considers agents' heterogeneous characteristics, making it suitable for analyzing situations in which agents have varying decision-making abilities and interact in complex ways. The use of ABMs in housing market analyses provides interesting insights. For instance, Geanakoplos. Axtell, Farmer, Howitt, Conlee, Goldstein, Hendrey, Palmer, and Yang (2012) find that the 1997–2007 period of boom and bust in the housing market was largely due to changes in leverage rather than interest rates. Laliotis, Buesa, Leber, and Población (2020) use an ABM to evaluate how regulatory caps on the loan-to-value ratio impact the economy. The use of ABMs in housing market analyses has evolved recently through the incorporation of spatial components. The location of a house is a significant factor in its valuation because amenities in its vicinity, such as hospitals, metro stations, and supermarkets, can impact its value markedly (Beynier, Maudet, Rey, and Shams, 2021). Evans, Glavatskiy, Harré, and Prokopenko (2023) construct a large urban housing ABM to simulate the Sydney housing market. By adopting graph theory, they incorporate spatial factors into their model. Our study also models the difference in value based on the locations of houses by adding housing into the Sugarscape model. Housing in areas with abundant resources is evaluated as having a higher value. Furthermore, investors may have different information depending on their relative housing locations, leading to the creation of heterogeneous expectations. To analyze the impact of heterogeneous expectations on the housing-price cycle, we extend the Sugarscape model using an ABM.

3. Methodology

3.1. Sugarscape model for the housing market

This study uses the Sugarscape model to construct an ABM for the housing market.[1] The following is an overview of the basic form of the Sugarscape model. The Sugarscape model is defined as a two-dimensional grid. Each patch is assigned the maximum sugar value (*max-sugar*). Agents acquire the sugar on their patch and consume some unit of that sugar to remain alive. During the simulation, they move to the patch with the highest sugar among nearby patches. Once consumed, each patch replenishes its sugar.

***Key Assumptions for the Sugarscape Model*:**

i) Sugar is piled on patches in the grid world.

ii) Agents move to a patch with the highest sugar among nearby patches.

iii) Agents consume the sugar located on the patch.

[1] We use *Netlogo*, which is designed to simplify the implementation of ABMs (Wilensky, 1999). We refer to the Sugarscape models in the library provided by *Netlogo* (Li and Wilensky, 2009a, 2009b, 2009c).

iv) After consumption, sugar is regenerated gradually.

We expand the Sugarscape model by incorporating houses. In the original Sugarscape model, agents remain on the patch in which they acquire sugar. However, in our model, agents return to their homes to rest after seeking sugar. Agents consume sugar once they seek rest in their homes. This assumption causes agents' sugar yield to vary depending on the locations of their houses. The differences in yield between houses make them worth different amounts. Agents want to move to houses with higher yields, which naturally leads to house trading. We assume that houses are traded through auctions and observe how housing prices change by varying how agents form expectations of house prices. In our model, sugar functions as the currency for trading houses.

***Assumptions about Housing in the Sugarscape Model*:**

i) Agents return to their houses to rest after collecting sugar.

ii) Agents want to move to houses with higher yields.

iii) Houses are traded through auctions.

A detailed description of the proposed model is provided below. We describe how we set up the initial situation in the model and explain how agents harvest sugar and trade houses.

3.2. Initial settings

In this section, we outline the initial settings for our simulation, which is based on a 50-by-50 grid world, as illustrated in Panel A of Figure 1. This grid world serves as the foundation for our adaptation of the Sugarscape model, as suggested by Epstein and Axtell (1996). In the initial stage, sugar accumulates to its maximum capacity on each patch. The color depends on how much sugar has accumulated on the patch; the darker the color, the more sugar has accumulated on that patch. Thereafter, houses and agents are generated. Consider an economy with N agents and H houses ($N < H$). To ensure stable simulation results, the number of agents and houses are fixed throughout the simulation process. Houses are created using random patches. We randomize the initial locations of houses to be independent of the distribution of sugar following the classical Sugarscape model. Even if the initial locations of houses are randomized, we can predict that the distributions of houses become similar to that of sugar as the simulation progresses because agents prefer to live in houses close to patches with more sugar. We assume that sugar is not generated on patches on which houses are located.

Figure 1. A Snapshot of the Sugarscape Model

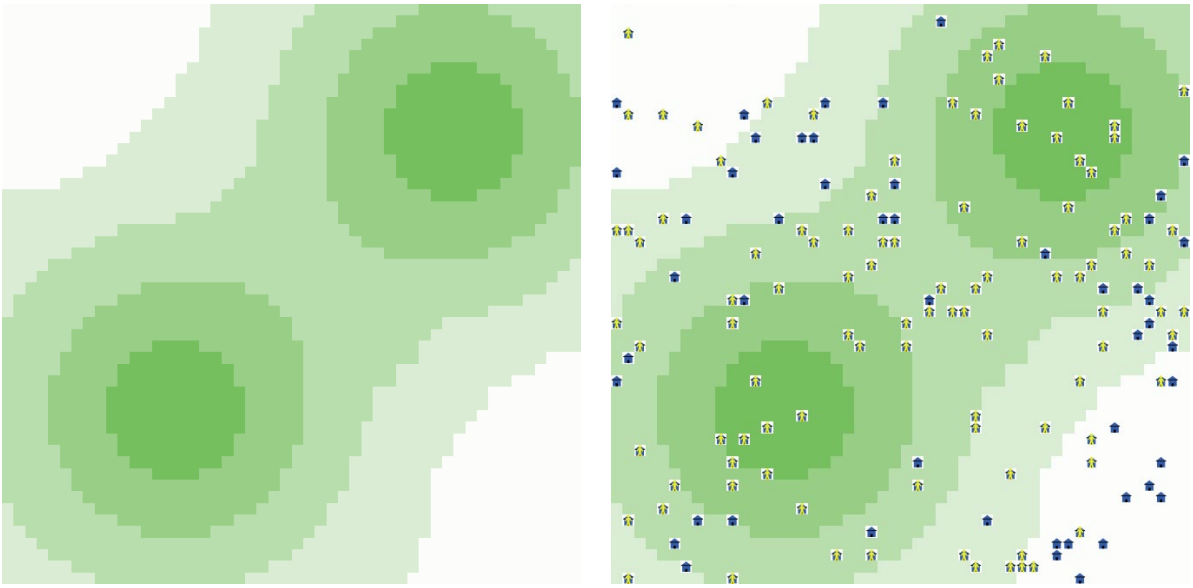

Panel A. Patch setting

Panel B. Agent setting

Note: This figure depicts the Sugarscape model's initial settings. Panel A shows the patch setting in the Sugarscape model. The grid world comprises 50-by-50 patches in both panels. The darker the color of the patch, the more sugar is on that patch. In Panel B, people and houses are randomly located. People are represented by yellow person icons and houses are represented by blue house icons.

After houses are built, agents are born in those houses and assume ownership of them. The ownership of houses in which no agents are born is assigned randomly to agents. If an agent owns a house but does not live there, it can be considered as they rent it to someone else. Because we are only modeling transactions between homeowners, we do not need to consider the decisions of renters. Therefore, renters are not represented in the model. If a house remains occupied, it is not demolished. However, houses that remain unoccupied for a certain period, which is set to 10 steps in our simulation, are demolished. Thus, these assumptions are valid. A house with a long-lived occupant is likely to have a high value; therefore, it continues to be maintained to prevent deterioration. Alternatively, this could be interpreted as occupants rebuilding on the same spot on which the house is deteriorating. In our model, the value of a house is determined by its location; therefore, it is reasonable to assume that agents have no incentive to change the location of their current residence. On the contrary, since unoccupied houses have a relatively low value, it is not too far-fetched to assume that when a house becomes obsolete, it is demolished and a new house is built elsewhere.

To maintain a constant number of houses, we adopt a system where a new house is constructed each time an existing house is demolished. Importantly, the owner of the demolished house becomes the owner of the new house. When agents are first created, they receive a sugar endowment, and their maximum lifespan is randomly assigned between 60 and 100. An agent dies when they have insufficient sugar to consume or reach the maximum age. To maintain a constant number of agents throughout the economy, a new agent is introduced for every agent that dies.

The new agent inherits the assets of the dead agent (i.e., sugar and houses). Agents and houses are located randomly, as shown in Panel B of Figure 1. In the classical Sugarscape model, agents gather on patches with high *max-sugar*. To determine whether a similar phenomenon is observed in our model, we measure the population density around the fertile area using the cost function of *K*-means clustering. *K*-means clustering is a machine-learning method that aims to find the core in which the data are clustered. The goal of this method is to identify the cores in each dataset with the smallest average distance from the core. In this study, the clustering level is calculated by referring to the cost function used in this methodology. Two cores can be set in the model in which agents cluster on a patch with a high maximum sugar amount, as shown in Figure 2.

Figure 2. Location of the Cores in the Sugarscape Model

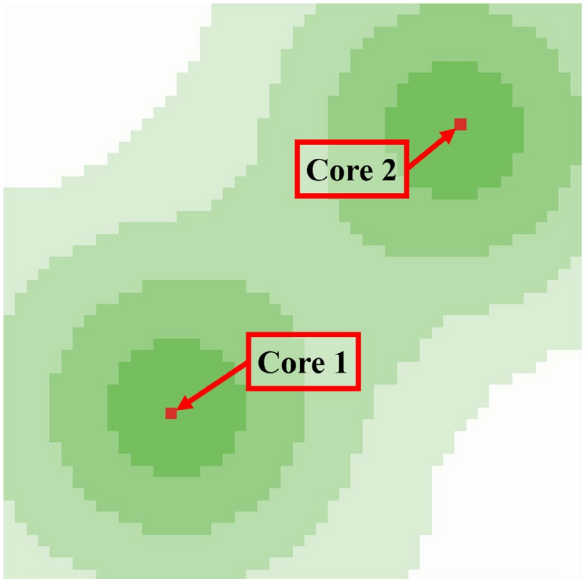

Note: This figure depicts the locations of two cores. The grid world comprises 50-by-50 patches. The darker the patch color, the more sugar is accumulated. Red patches are the cores in the middle of patches on which the most sugar is accumulated.

The distance between the two cores for each agent at step t ($d_{n,t}^{(c)}$) is calculated using Equation (1). $x_{n,t}$ and $y_{n,t}$ are the x and y coordinates of agent n at time t, respectively. x_c and y_c are the x and y coordinates of each core, respectively.

$$d_{n,t}^{(c)} = \sqrt{\left(x_{n,t} - x_c\right)^2 + \left(y_{n,t} - y_c\right)^2} \quad (1)$$

n: Index of agents

c: Index of each core, $c = 1,\ 2$

The clustering level at time t (D_t) is the average of the distances on the closer side of the two cores and is calculated using Equation (2). N denotes the number of agents. The lower the clustering level, the greater the number of agents living around a core.

$$D_t = \frac{1}{N}\sum_{n=1}^{N} \min\left\{d_{n,t}^{(1)}, d_{n,t}^{(2)}\right\} \quad (2)$$

3.3. Agent behaviors

Agents are located in their residences at the beginning of each step and leave them to earn sugar. They move to the patch with the highest payoff among the patches in their field of vision and acquire sugar. The payoff for each patch is the amount of sugar on the patch minus the movement cost. $m_{v,t}$ is the amount of sugar accumulated on patch v at time t and $d_{i,t}^{(v)}$ is the distance to patch v from house i. θ is a moving cost parameter. Because agents must leave their residences, obtain sugar from a patch, and return, the movement cost is counted twice. Therefore, the payoff of patch v at time t ($\pi_{i,v,t}$) is calculated as in Equation (3).

$$\pi_{i,v,t} = m_{v,t} - 2\theta \cdot d_{i,t}^{(v)} \quad (3)$$

Agents' spatial information is constrained by their visual range, as in the classical Sugarscape model. The field of vision is the extent to which agents can acquire information regarding the amount of sugar. In our model, agents' yield and the values of their houses are established based on the sugar levels of adjacent patches. Therefore, it is crucial for agents to search adjacent patches to determine the sugar of each patch to optimize their decision-making. Figure 3 illustrates the visible areas centered on agents *n* and *i*. The patches inside the dotted lines are visible.

Figure 3. Field of Vision

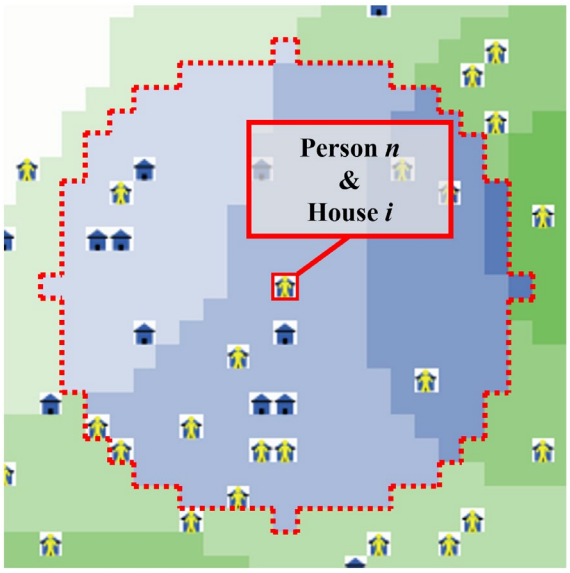

Panel A. When person *n* is the owner of the house *i*

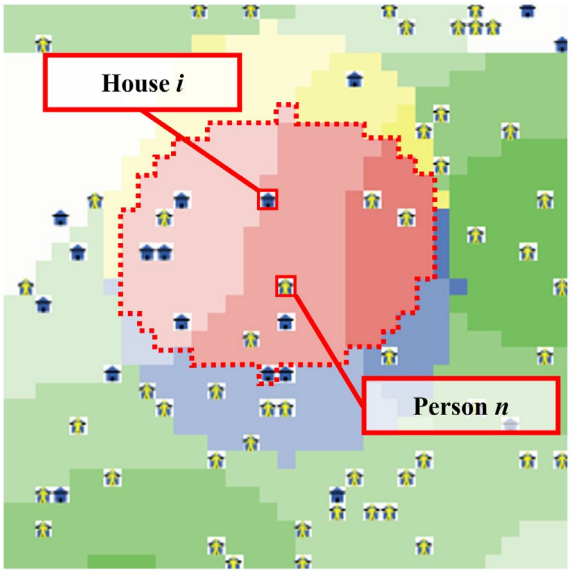

Panel B. When person *n* is not the owner of the house *i*

Note: These figures depict people's field of vision. In both panels, the grid world comprises 50-by-50 patches. The darker the patch's color, the more sugar is accumulated. In both panels, people are represented by yellow person icons, and houses are represented by blue house icons. Panel A presents a person *n*'s field of vision when person *n* is the house *i*'s owner. The area inside the red dotted line is the range that person *n* can observe for house *i*. Panel B depicts a person *n*'s field of vision when person *n* is not the owner of house *i*. The area inside the red dotted line is the range that person *n* can observe for house *i*.

As shown in Panel A, when agent *n* owns house *i*, agent *n* can observe all the patches in the house *i*'s field of vision. Thus, the payoff that the agent in house *i* can receive at time *t* is the highest value among $\pi_{i,v,t}$ in the vision set (V_i). The payoff ($\pi_{i,t}$) can be summarized as

$$\pi_{i,t} = \max_{i \in V_i} \pi_{i,v,t} \tag{4}$$

V_i: Vision set of house *i*

Agents are assumed to know all the possible information regarding their own houses. However, they do not know all the information regarding houses that they do not own. Agents must determine the amount of sugar on the patches around a house to evaluate it; however, they cannot explore all the surroundings of houses that they do not own. Therefore, they can obtain information about the space in which their vision set and the house's vision set overlap. Panel B depicts the information agent *n* can obtain when pricing house *i*. After the earning process, agents

decide on houses: *i*) whether to sell their houses or buy other houses nearby and *ii*) which of their houses to live in. Agents trade houses through auctions. We assume that all vacant houses are included in these auctions. Agents estimate the values of houses in their field of vision and predict their prices. If the expected potential payoff of a house is higher than the expected price, agents bid for that house at the auction. This is inspired by the auction model in game theory. If players have different valuations of the auction item and do not know the valuations of others, it is efficient to bid at a price equal to their own valuation.

Sellers compare the bidding prices of buyers and trade at the highest value, while ensuring that the trade price surpasses their reserve price. To determine the reserve price, sellers choose the higher value between the expected potential payoff and the expected house price. The reserve price represents the opportunity cost of selling the house. The potential payoff refers to the value of residing in the house in the future, whereas the expected price denotes the value of selling the house in the future. If the potential payoff is greater than the bidding price, the seller is motivated to profit from the property. If the expected price exceeds the bidding price, the seller is interested in passing on the present transaction and trading in the future period. Thus, it can be inferred that the seller will only opt to sell if the bidding price is higher than both the potential payoff and the expected price. Additionally, we assume that the reserve price decreases proportionally to the length of time a house remains vacant. This is because houses age and are eventually demolished over time, and owners may feel a sense of urgency to sell their houses before they are demolished. During auctions, it is essential for agents to estimate the potential payoff (i.e., value) and predict house prices. Below is a detailed explanation of how to estimate housing values and predict prices. The potential payoff of a house is determined based on the sugar on the patches around the house. Agents can calculate their houses' payoff at time *t* as in Equation (4). However, determining the exact amount of sugar that can be collected at the beginning of a step is challenging because sugar on surrounding patches fluctuates according to the order of agents' movements. Therefore, the house *i*'s expected payoff can be summarized as $\overline{\pi}_{i,t}$, which is the average of the payoffs of all the patches in the vision set (V_i).

$$\overline{\pi}_{i,t} = \frac{1}{n(V_i)} \cdot \sum_{v \in V_i} \pi_{i,v,t} \tag{5}$$

As agents can continue collecting payoffs while they are in a house, the potential payoff is calculated by considering the value that can be obtained in the future. When the discount rate is ρ, the potential payoff of house *i* at time *t* ($\Pi_{i,t}$) can be calculated as in Equation (6).

$$\Pi_{i,t} = \sum_{\tau=0}^{\infty} (1-\rho)^{\tau} \cdot \overline{\pi}_{i,t+\tau} \tag{6}$$

To accurately calculate $\Pi_{i,t}$, all the payoffs that will occur in the future must be known, which is practically impossible. At time *t*, all the future payoffs of house *i* that will occur are assumed to be $\overline{\pi}_{i,t}$. Therefore, the expected potential payoff of house *i* estimated at time *t* ($E\left[\Pi_{i,t}\right]$) is calculated as in Equation (7).

$$E\left[\Pi_{i,t}\right] = \sum_{\tau=0}^{\infty}(1-\rho)^{\tau} \cdot \overline{\pi}_{i,t} = \frac{1}{\rho} \cdot \overline{\pi}_{i,t} \quad (7)$$

As agents possess limited information regarding houses that they do not own, they cannot accurately know the average payoff of house *i* ($\overline{\pi}_{i,t}$). Therefore, agent *n* estimates $\pi_{i,t}$ based on the payoffs of the patches in the intersection between agent *n*'s vision set and house *i*'s vision set ($V_{i,n} = V_n \cap V_i$).

$$E_n\left[\overline{\pi}_{i,t}\right] = \frac{1}{n(V_{i,n})} \cdot \sum_{v \in V_{i,n}} \pi_{i,v,t}, \quad (8).$$

Agent *n* estimates all the future payoffs of house *i* that will occur as $E_{n,t}\left[\overline{\pi}_{i,t}\right]$; hence, the expected potential payoff of house *i* estimated by agent *n* ($E_n\left[\Pi_{i,t}\right]$) is presented in Equation (9).

$$E_n\left[\Pi_{i,t}\right] = E_n\left[\sum_{\tau=0}^{\infty}(1-\rho)^{\tau} \cdot \overline{\pi}_{i,t+\tau}\right] = \sum_{\tau=0}^{\infty}(1-\rho)^{\tau} \cdot E_n\left[\overline{\pi}_{i,t}\right] = \frac{1}{\rho} \cdot E_n\left[\overline{\pi}_{i,t}\right] \quad (9)$$

Agents participate in the auction by considering the expected potential payoff, defined in Equation (9) as an estimate of the value of the house. Agents use historical prices to forecast future prices. If all agents possessed identical knowledge about houses (i.e., the amount of sugar distributed around those houses), house prices would be equivalent to the actual house values. However, in our model, agents hold limited data on houses, making it challenging for them to predict whether a house price will match its estimated value. Therefore, we posit that agents forecast future housing prices based on past transaction prices, rather than on their own appraisals of value. However, the infrequent trading of houses poses a challenge for precise forecasting using past prices. If the house that an agent intends to purchase has not been traded for an extended period, it becomes even more difficult to ascertain its current price. To address these challenges, we propose incorporating the housing price index (HPI) into our model. The HPI is an aggregate of house prices traded at each stage that is publicly accessible to all agents. This allows agents to estimate market-wide changes in house prices and use it to predict the approximate price of the house they intend to trade. This process is described next. The assumptions regarding house pricing are as follows. The price of a house is determined through the auction. If house *i* is traded at time *t*, then the trade price ($P_{i,t}^{r}$) is recorded as the price of house *i* in period *t*. If house *i* is not traded, its price ($P_{i,t}^{e}$) is considered to have changed because of HPI returns (r_t), as defined in Equation (10). This assumption highlights how price fluctuations in the market can affect individuals' expectations of price fluctuations for specific houses.

$$P_{i,t} = P_{i,t}^{r} \cdot I_{H_t}(i) + P_{i,t}^{e} \cdot \left(1 - I_{H_t}(i)\right) \quad (10)$$

H_t: Set of houses traded in step t

$I_{H_t}(i)$: When $i \in H_t$, $I_{H_t}(i) = 1$. Otherwise, $I_{H_t}(i) = 0$.

$P_{i,t}^r$: Price of house *i* traded at time *t*

$P_{i,t}^e = (1 + r_t) \cdot P_{i,t-1}$: Estimated price of house *i*, which did not trade at time *t*

To calculate the HPI, prices are indexed to a reference point. The transaction price is affected by the value of the traded house; however, if we simply calculate the HPI from the transaction price, we run the risk of overestimating price changes in the market. This is because on one day, only low-value houses may have been traded, resulting in a very low HPI. By contrast, on the next day, only high-value houses may have been traded, making it seem like the market suddenly changed. Therefore, we calculate how much the price has changed based on the initial value of the house and the HPI accordingly. We define house *i*'s price ratio from the initial value at time *t* ($R_{i,t}$) using Equation (11). $\Pi_{i,*}$ means the initial potential value of house *i*, which can be calculated following Equations (3)–(6).

$$R_{i,t} = \frac{P_{i,t}}{\Pi_{i,*}} \times 100 \tag{11}$$

The HPI is defined as the average value of the price ratio of traded houses ($R_{i,t}$, $i \in H_t$). The HPI at time t (h_t) is calculated using Equation (12). We define the log return of the HPI in Equation (13).

$$h_t = \frac{1}{n(H_t)} \sum_{i \in H_t} R_{i,t} \tag{12}$$

$$r_t = \ln(h_t) - \ln(h_{t-1}) \tag{13}$$

$n(A)$: Number of elements in set A

$R_{i,t}$: Price Ratio

Agents can forecast future prices on the basis of previous prices by predicting the rate of return at time *t*. When $E_n[r_t]$ is the HPI returns estimated by agent *n*, the expected price is computed using Equation (14).

$$E_n\left[P_{i,t}\right] = (1 + E_n[r_t]) \cdot P_{i,t-1} \tag{14}$$

Agents predict future returns based on past returns. Although numerous factors can be considered, we simplify the factors that impact an agent's prediction using the expectation parameter. Subsequently, the expectation is represented by Equation (15). η_n is the agent n's expectation parameter. Individuals may hold differing opinions about future price fluctuations, with varying values of η_n. We assume that agents' expectation parameter follows a uniform distribution between $-h$ and h ($\eta_n \sim Uniform(-h, h)$), where $h \geq 0$ denotes the heterogeneity level.

$$E_n[r_t] = r_{t-1} + \eta_n, \tag{15}$$

If $h = 0$, then all agents are expected to be homogeneous. However, as h increases, agents have different expectations of housing prices. The expectations of HPI returns significantly influence the model's outcomes. Thus, we classify the expected return into two categories.

(a) *Homogeneous expectations*: Agents expect today's return to mirror the previous one. Thus, all agents believe $E_n[r_t] = r_{t-1}$ (i.e., $h = 0$).

(b) *Heterogeneous expectations:* Individuals hold homogeneous beliefs. If η_n is widely distributed (i.e., $h > 0$), agents hold different beliefs regarding future housing prices.

The discrepancy between these two assumptions indicates the effect of heterogeneous expectations on the housing market. Therefore, we experiment with and observe how these two assumptions lead to different simulation results.

4. Simulation Results

4.1. Experimental design

We examine the influence of limited information and agents' heterogeneous expectations on housing-price dynamics. We conduct experiments by altering the size of the agents' vision set (V_n) and heterogeneity (h) to explore how vision and heterogeneity affect system volatility. We use two metrics to measure volatility. The first is the Hodrick–Prescott (HP) filter. The HP filter is an econometric technique that segregates the trend and cycle components by smoothing time-series data (Yu and Ryu, 2020). The separate trend and cycle components can provide insights into how vision and heterogeneity impact housing prices. A guideline exists for smoothing the parameters of the HP filter based on the periodicity of the data. Because we use simulated data, we require an assumption about the data frequency. In our model, each step represents a cycle in which people consider trading houses. As housing is unlikely to have short trading cycles, we assume that one step of our simulation covers the sufficiently long time horizon of one year. Thus, we set the smoothing parameter (λ) to 100 following the guideline for the HP filter. Second, we analyze the distribution and standard deviation of HPI returns. By calculating how often HPI returns have extreme values and how large the standard deviation is, we can measure housing price volatility.

For these experiments, we simulate the model described in Section 3. Table 1 lists the detailed parameter settings used in the simulations.

Table 1. Parameter Settings

Patches	
Max-sugar	1 ~ 4
Houses	
Number-of-houses (H)	150
Max-empty-days	10
Agents	
Number-of-agents (N)	100
Discount-rate (ρ)	0.01
Initial-endowment	30
Consumption	1
Vision	5, 10, 15, 20, 25
Max-age	60 ~ 100
Heterogeneity (h)	0, 10^{-3}, $10^{-2.5}$, 10^{-2}, $10^{-1.5}$, 10^{-1}, $10^{-0.5}$, 1, $10^{0.5}$, 10, $10^{1.5}$, 10^{2}

In the simulation, we set the seed number of the random generator built into *NetLogo* from 1 to 100 and run the simulation 100 times, with each simulation comprising 500 steps. We simulate three expectation assumptions and compare the results. By comparing cases with the same seed number, we can infer how the expectation assumption affects the results in the same initial setting.

4.2. Vision

As the simulation progresses, the shape of agents' migration is highly dependent on their vision. Figure 4 shows the agents' and houses' locations after 500 steps, according to the agents' vision. To observe a consistent result, the random seed number is fixed at 1 and agents' expectations are heterogeneous (h = 1). Panel A shows the initial locations of agents and houses. The other panels show the results when the vision of the agent is set differently.

Figure 4. Clustering by Vision

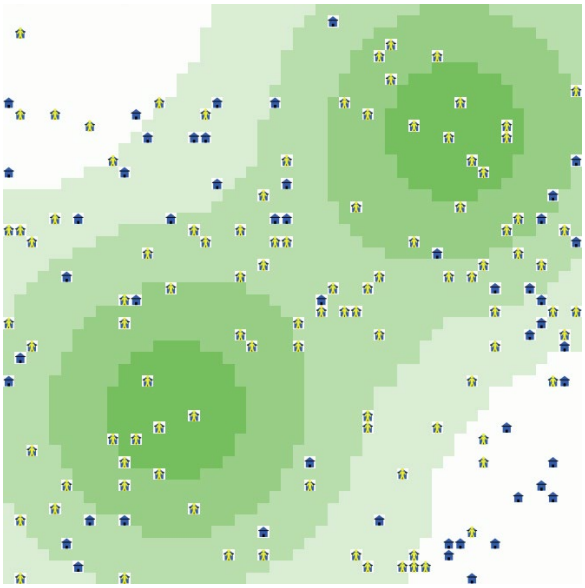

Panel A. Initial locations

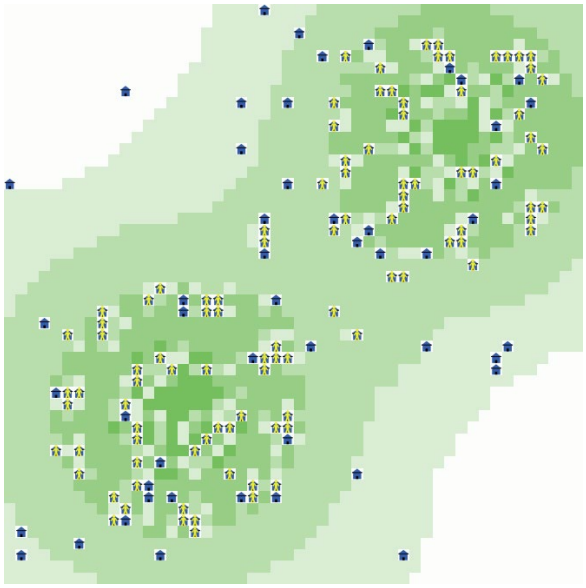

Panel B. *Vision* = 5

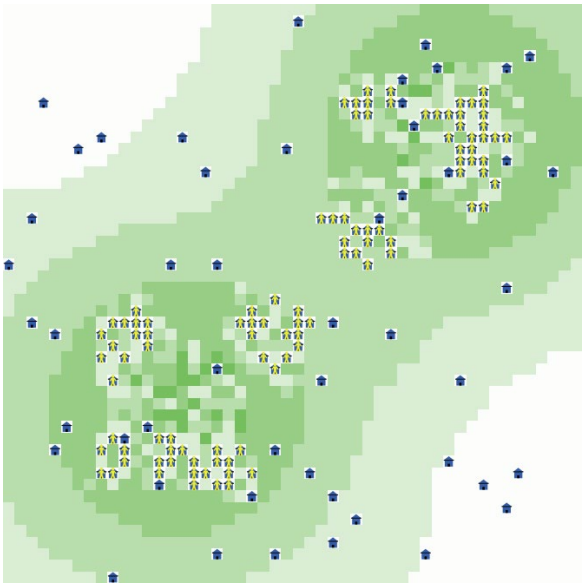

Panel C. *Vision* = 10

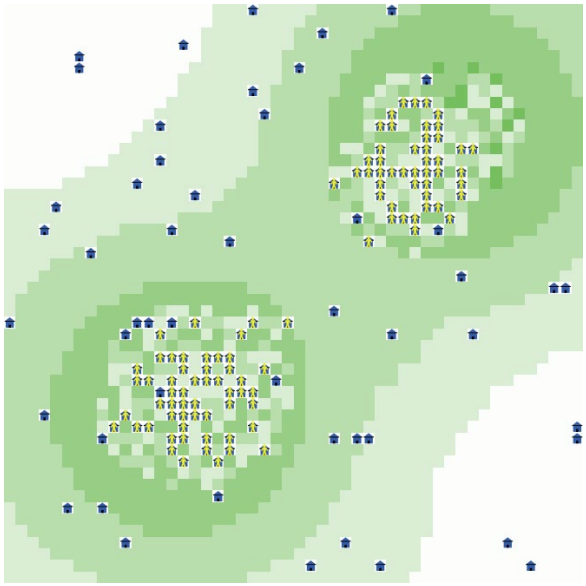

Panel D. *Vision* = 15

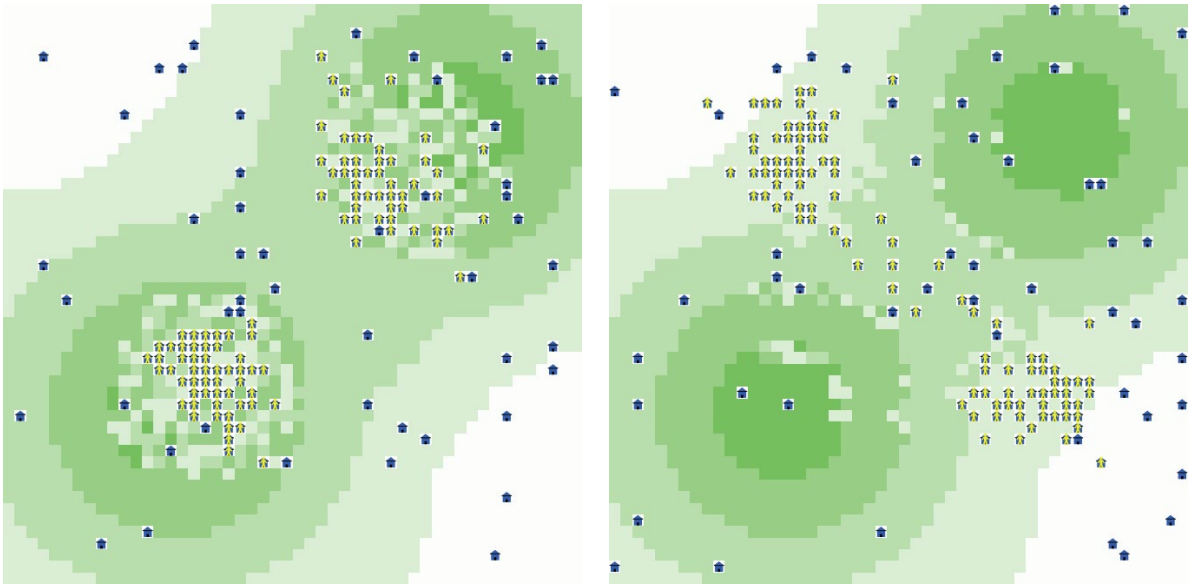

Panel E. Vision = 20 *Panel F. Vision* = 25

Note: This figure depicts the changes in people's locations to agents' vision. The random seed number is fixed at 1. Agents' expectations are 1. The grid world comprises 50-by-50 patches. The darker the patch's color, the more sugar is accumulated. In each panel, houses are represented by blue house icons, and agents are represented by yellow person icons. Panel A depicts the initial locations of people and houses. The other panels illustrate the different locations after 500 steps based on the assumptions regarding people's vision (*Vision* = 5, 10, 15, 20, and 25).

While the locations vary by vision, Panels B, C, D, E, and F of Figure 4 show agents clustered in certain areas. The convergence toward clustering represents a general trend of individuals gravitating toward city centers. This outcome aligns with the spatial distribution patterns observed in a modern economy, where approximately 80–90% of the population clusters in residential urban areas. Our model illustrates how this clustering pattern naturally emerges from an agent's locational choices and housing transactions. Conventionally, geographic clustering has been considered to be a result of the advantages of urban agglomeration such as economies of scale (Krugman, 1991) or learning (Duranton and Puga, 2004). In Panel B, we observe that when people's vision is 5, they cluster near two sugar-rich cores. Then, as shown in Panels C and D, when *Vision* reaches 10, they congregate slightly closer to the cores. However, in Panel E, where *Vision* is 20, they congregate slightly more toward the center of the grid world than the two cores. In Panel F, when *Vision* is 25, they are far from converging at the cores. Given that our grid world is 50-by-50, when *Vision* is 25, agents can obtain virtually all the information in the grid world and can obtain sugar from almost any patch that has sugar in the earning process. People seem to cluster near areas equidistant from the two sugar-rich cores. This pattern can also be observed at the clustering level. Figure 5 summarizes the clustering levels by *Vision*.

Figure 5. Clustering Levels by Vision

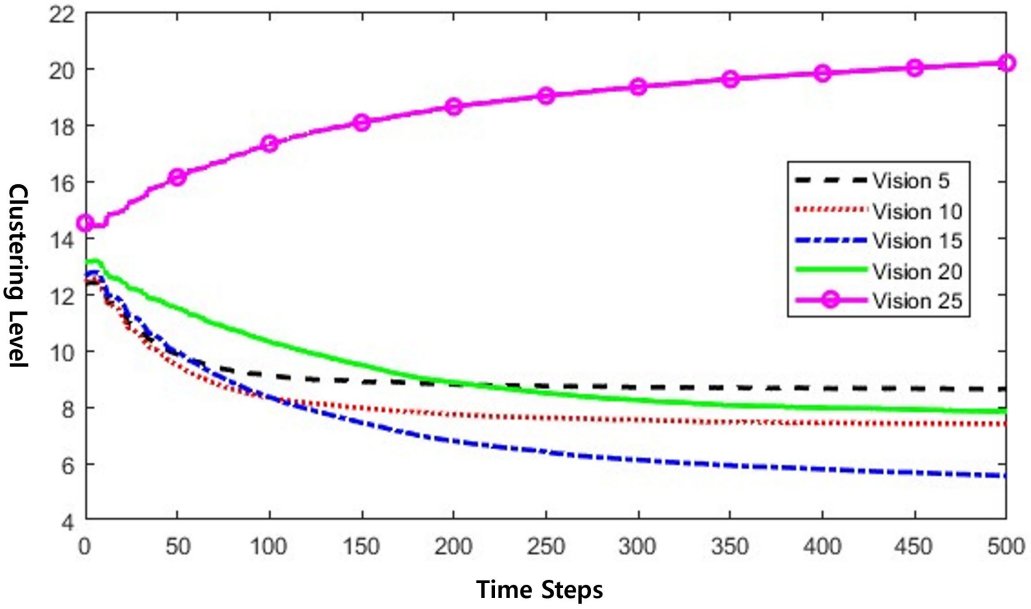

Note: This figure illustrates the average clustering levels for different visions. The horizontal axis represents time steps and the vertical axis represents the clustering level. The clustering levels are the average values over 100 runs. The dashed, dotted, dash-single dotted, solid, and circled lines indicate *Vision* = 5, 10, 15, 20, and 25, respectively.

Figure 5 shows the average clustering level at each step over 100 runs. The case with *Vision* = 15 manifests in agents clustering closest to the cores in the final step, with values of 5, 10, and 20 following closely. However, the speed at which the steady state is reached appears to differ. Generally, the lower the vision, the faster the steady state is achieved. At visions of 5, 10, 15, and 20, clustering levels gradually decrease. However, at *Vision* = 25, the clustering level increases over time. Panel F of Figure 4 supports this finding. It can be inferred that agents are more knowledgeable about the patches and can access them for sugar. Therefore, they prefer to be located where they can simultaneously reach the two sugar-rich cores at equal distances, ultimately leading them to move away from the cores over time. As agents' locations are affected, so too are the HPI dynamics. Figure 6 illustrates how these dynamics change as agents' vision alters.

Figure 6. HPI by Vision

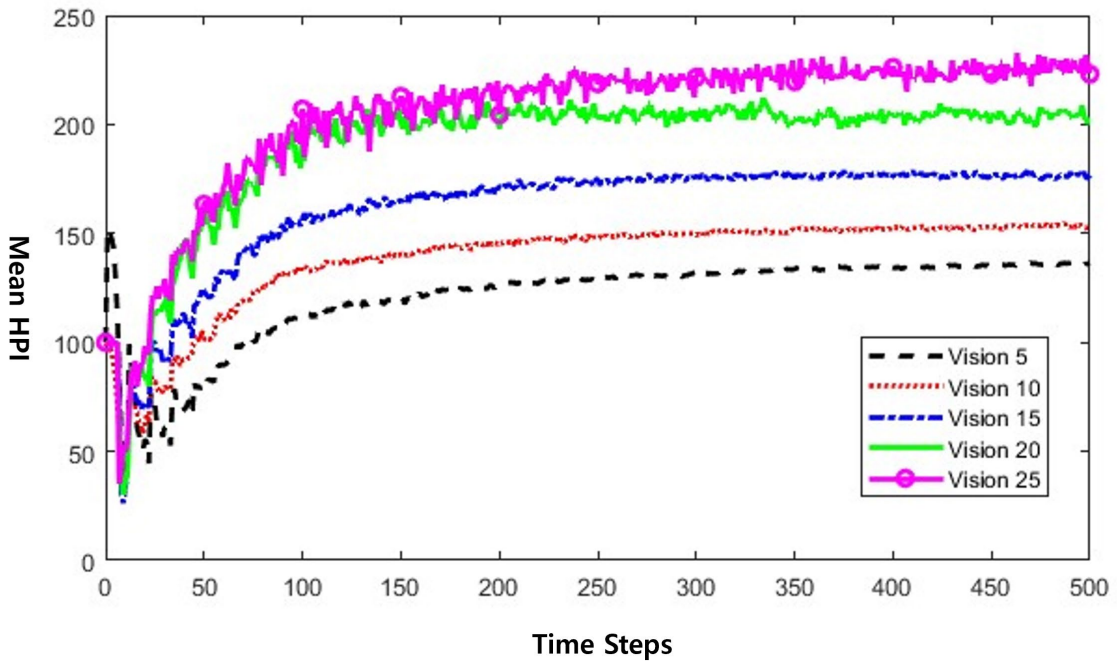

Note: This figure illustrates the average HPI for different visions. The horizontal axis represents time steps and the vertical axis represents the HPI. The HPIs are average values over 100 runs. The dashed, dotted, dash-single dotted, solid, and circled lines indicate *Vision* = 5, 10, 15, 20, and 25, respectively.

The HPI values shown in Figure 6 are averaged over 100 runs in a stepwise manner. Despite the variance in *Vision* values, a consistent pattern of the HPI converging to a specific value is observed after approximately 100 steps. Moreover, as the value of *Vision* increases, so does the average HPI. Additionally, with an increase in *Vision*, there appears to be a larger fluctuation in the HPI. To corroborate these results, we employ the HP filter to divide the HPI into its trend and cycle components. Panel A of Figure 7 shows the average trend components computed over 100 runs. Because the amplitude of the cycle is considered to be more important than its direction, we calculate the average absolute value of the cycle component in Panel B.

Figure 7. Trend and Cycle Components by Visions

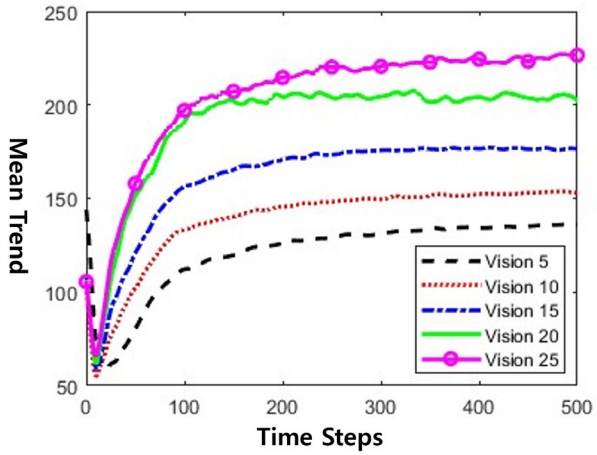

Panel A. Mean of the trend components

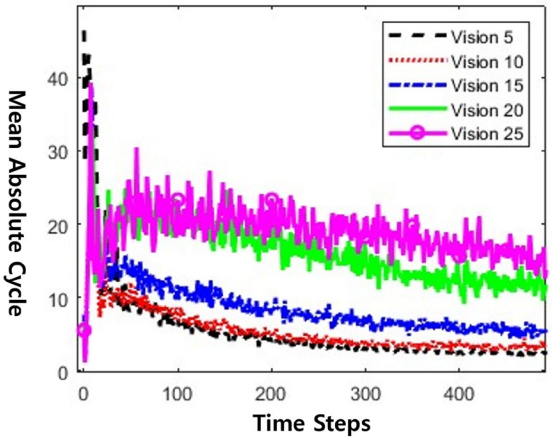

Panel B. Mean of the absolute cycle components

Note: This figure illustrates the average HPI for different visions. The horizontal axis represents time steps and the vertical axis represents the trend and cycle components of the HPI. The HPIs are the average values over 100 runs. The dashed, dotted, dash-single dotted, solid, and circled lines indicate *Vision* = 5, 10, 15, 20, and 25, respectively.

Panel A of Figure 7 shows an initial drop in the HPI followed by a subsequent rise. This is likely because we randomized the initial locations of agents and houses. Initially, agents and houses are randomly distributed, leading to a lack of efficient housing transactions. As the vacancy period increases, the perceived value of these houses declines. Consequently, house prices gradually decline during this stage. However, as individuals migrate toward areas with abundant amenities, the proximity between agents increases. This proximity intensifies competition in the housing market, resulting in a sudden and sharp increase in property prices. This also explains the large initial variation in the cycle components shown in Panel B of Figure 7. In Panel A of Figure 7, the rate of the HPI increase slows at approximately 100 steps and converges to one value, regardless of the agent's vision. Figure 6 shows the correlation between a wider agent vision and a higher HPI trend. Panel B presents an upward trend in the cycle amplitude as agents' vision increases. In other words, the wider the field of vision of the agent, the more the HPI oscillates around high values. These findings are supported by the distribution of HPI returns in Figure 8. The histogram displays HPI returns categorized by vision and is the average of 100 runs.

Figure 8. Histogram of HPI Returns by Vision

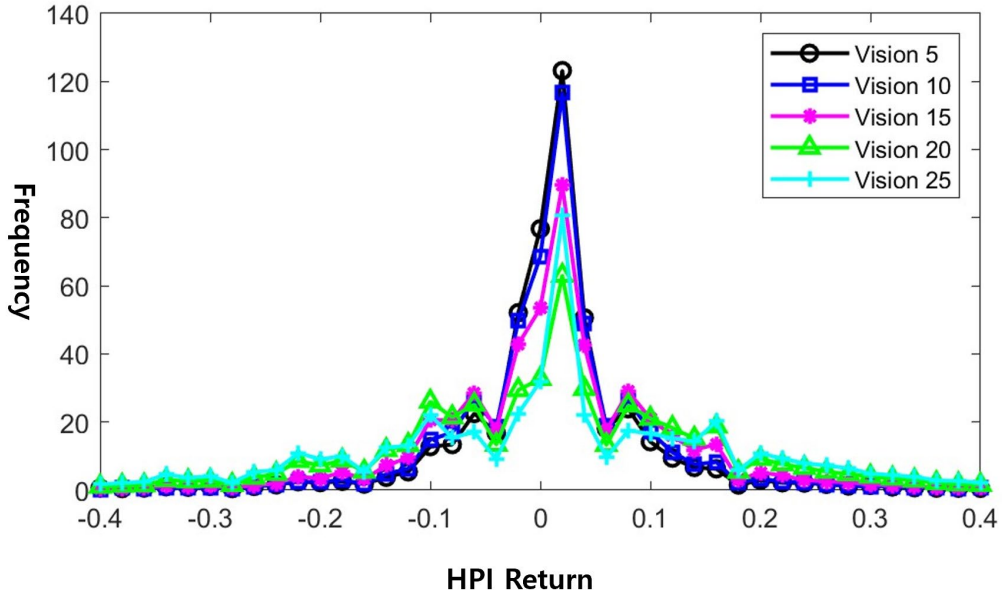

Note: This figure shows the distribution of HPI returns by vision in a histogram format. The horizontal axis represents the HPI return bins and the vertical axis represents the frequency. The frequency is the average value over 100 runs. The lines with circles, squares, asterisks, triangles, and cross-markers correspond to *Vision* values of 5, 10, 15, 20, and 25, respectively.

Figure 8 illustrates that HPI returns follow a bell-shaped distribution, similar to a normal distribution. The distribution of returns appears to cluster more closely around the mean when *Vision* has a lower value and the tail becomes thicker as *Vision* increases. Higher *Vision* values indicate a higher likelihood of observing sudden increases or decreases in HPI prices. Figure 9 shows that the standard deviation of HPI returns varies with *Vision*. We average the standard deviation of HPI returns calculated from 100 trials and display it as a circular marker.

Figure 9. Standard Deviation of HPI Returns by Vision

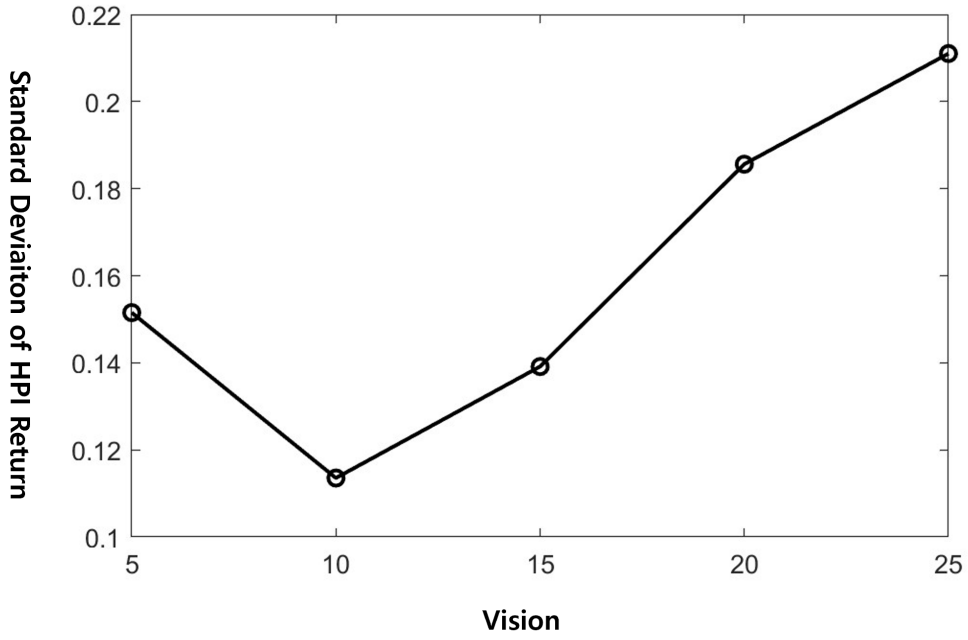

Note: This figure displays the correlation between the vision and standard deviation of HPI returns. The horizontal axis represents vision and the vertical axis denotes the standard deviation of HPI returns. Each point on the graph is the mean of 100 iterations.

In Figure 9, the standard deviation of HPI returns is at its minimum when *Vision* = 10 and displays an upward trend as *Vision* increases. These findings align with those shown in Figures 6–8. An agent's vision limits the information available on their work and housing auctions. If vision is excessively limited, an agent born in such an infertile location cannot obtain any sugar; moreover, their houses are too low in value to be traded. However, if an agent's vision is excessively broad, competition for work and house auctions may become overheated. In our model, housing transactions operate through an auction system with buyers bidding on prices and sellers settling the transaction at the highest price. This can lead to a sharp increase in prices during high-demand competition. Agents' expectations amplify the price spike, indicating that greater vision leads to higher volatility in HPI returns.

4.3. Heterogeneous expectation

The heterogeneity of agents' expectations creates complex HPI dynamics through a feedback mechanism in which past HPIs influence future HPIs. In this section, we examine how the level of heterogeneity among agents impacts HPI dynamics. As presented in Section 4.2, the migration patterns of agents change based on their vision, which affects the amount of information they receive and, consequently, the HPI dynamics. Therefore, we control for Vision when analyzing the impact of the degree of heterogeneity on the HPI. In Figure 9, a Vision value of 10 results in the lowest standard deviation of HPI returns. Therefore, we set Vision to 10, while keeping all the

other settings consistent with those in Section 4.2. In this subsection, we compare the homogeneous and heterogeneous expectation cases. The former corresponds to $h = 0$ in Equation (15), whereas the latter corresponds to $h > 0$. In most of our experiments, we assume the heterogeneous expectation case to be when $h = 1$, except when evaluating how the heterogeneity level affects the standard deviation of HPI returns. Figure 10 shows the terminal locations of houses and agents.

Figure 10. Clustering by Expectation Heterogeneity

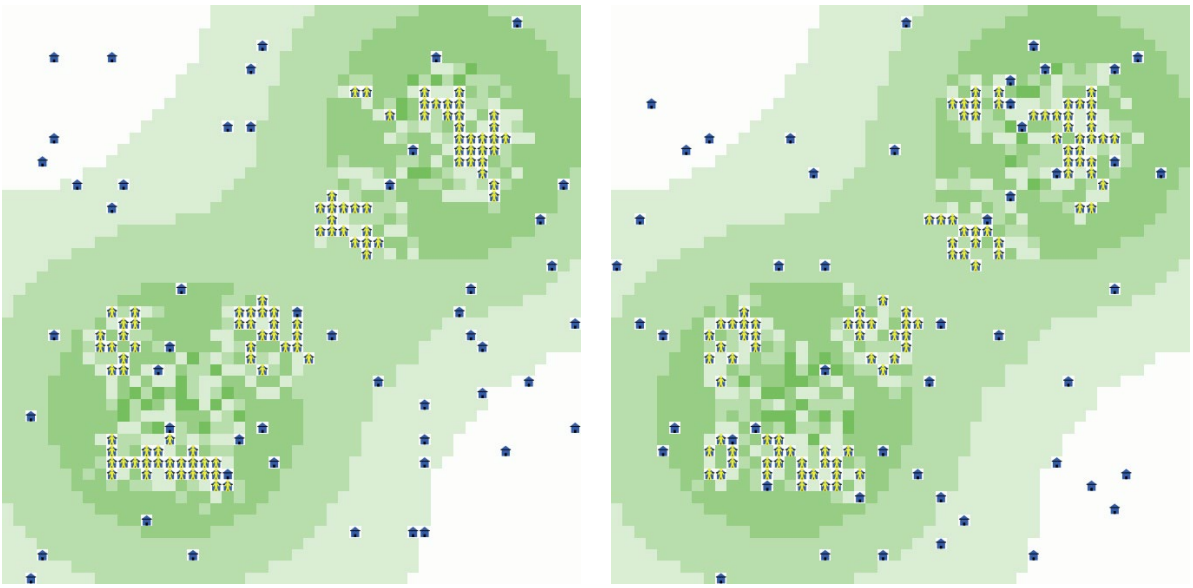

Panel A. Homogeneous expectations (h = 0)

Panel B. Heterogeneous expectations (h = 1)

Note: This figure depicts the changes in people's locations by the heterogeneity level of agents' expectations. The random seed number is fixed at 1. Agents' vision is 10. The grid world comprises 50-by-50 patches. The darker the patch's color, the more sugar is accumulated. In both panels, people are represented by yellow person icons, and houses are represented by blue house icons. Both panels illustrate the different locations after 500 steps based on the assumptions regarding people's expectations, namely, homogeneous expectations (h = 0) and heterogeneous expectations (h = 1), respectively.

The variance between the panels in Figure 4 appears to be insignificant. This implies that the impact of heterogeneity level on agent migration is less significant than that of vision. Nonetheless, it is crucial to monitor the change in clustering levels, as there may be dissimilarities in migration patterns, even if the position of the final step is the same. Figure 11 depicts the change in clustering levels over time. The clustering levels represent the average values of 100 runs.

Figure 11. Clustering Levels by Heterogeneity

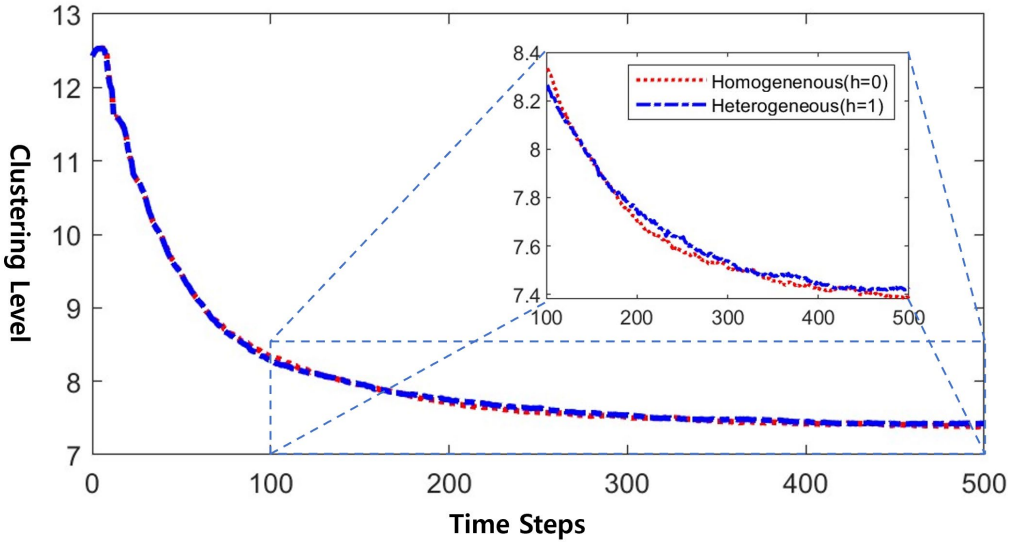

Note: This figure illustrates the clustering levels for the three cases. The horizontal axis represents time steps and the vertical axis represents the clustering level. The clustering levels are the average values over 100 runs. The dashed and dash-single dotted lines indicate homogeneous ($h = 0$) and heterogeneous ($h = 1$) expectations, respectively. The inset figure zooms in on the results after 100 steps.

The results shown in Figures 10 and 11 imply that agents follow similar migration patterns if they possess the same level of vision. When we analyze the impact of the heterogeneity level on the HPI in later experiments, it is safe to assume that no problems are caused by different migration patterns. Therefore, we do not consider migration patterns in the following analyses. To observe the impact of heterogeneity on HPI dynamics, we first examine the HPI dynamics in both the homogeneous and the heterogeneous expectation cases. Figure 12 illustrates the average HPI by heterogeneity. The HPI values are averaged over 100 runs.

Figure 12. HPI by Heterogeneity

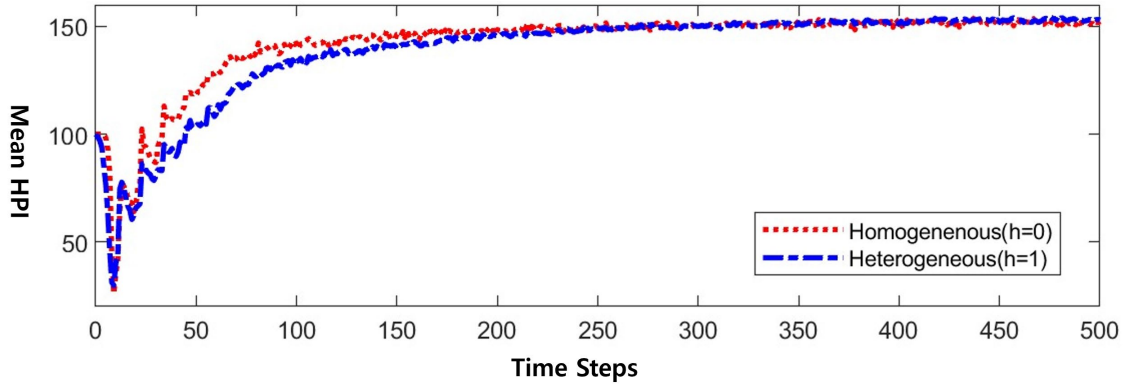

Note: This figure depicts the HPI data when the random seed number is 1. The horizontal axis represents time steps and the vertical axis represents the HPI. The HPIs are the average values over 100 runs. The dashed and dash-single dotted lines indicate homogeneous (h = 0) and heterogeneous (h = 1) expectations, respectively.

In both cases, the HPI reaches a similar steady state, but the homogeneous expectation case seems to increase at a faster rate than the heterogeneous expectation case. To explore these results in more detail, Figure 13 summarizes the results of decomposing the HPI into trends and cycles using the HP filter. Panel A shows the trend component averaged over 100 trials, whereas Panel B shows the absolute value of the cycle component averaged over 100 trials.

Figure 13. Trend and Cycle Components by Heterogeneity

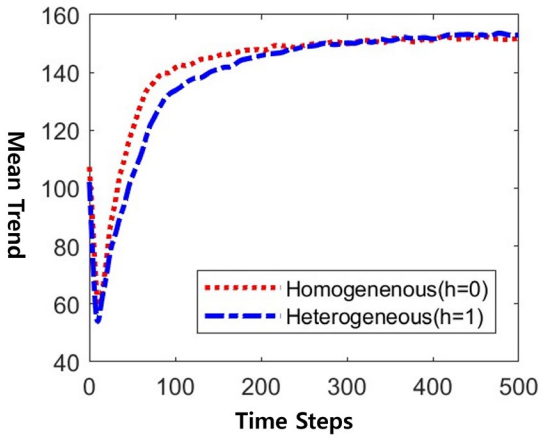

Panel A. Mean of the trend components

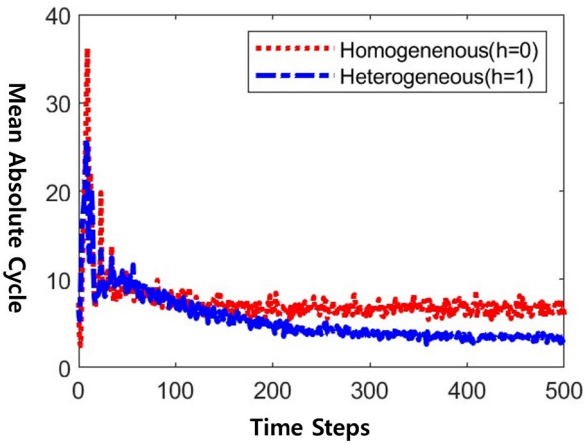

Panel B. Mean of the absolute cycle components

Note: This figure illustrates the average HPI for different heterogeneity. The horizontal axis represents time steps and the vertical axis represents the trend and cycle components of the HPI. The trend components are the average values over 100 runs. The cycle components are the average absolute values over 100 runs. The dashed and dash-single dotted lines indicate homogeneous (h = 0) and heterogeneous (h = 1) expectations, respectively.

As shown in Figure 7, large initial fluctuations are observed in Figure 13. As also shown in Figure 7, this initial fluctuation is likely due to the initial randomization. Panel A clearly shows that the HPI in the homogeneous expectation case increases faster than that in the heterogeneous expectation case. Panel B shows that the amplitude of the cycle component is higher in the homogeneous expectation case. This result implies that the more homogeneous agents' expectations of price changes, the larger the price changes. Under heterogeneous expectations, even if house prices rise, people predict a decrease or increase in house prices based on their expectations. When opposite expectations co-exist, the effect of price fluctuations is relatively small because the two groups neutralize each other's effects on prices during the transaction process. However, when considering homogeneous expectations, everyone predicts the same price

change, which causes prices to rise or fall. To determine how heterogeneity affects the HPI, Figure 14 shows the distribution of HPI returns.

Figure 14. Histogram of HPI Returns by Heterogeneity

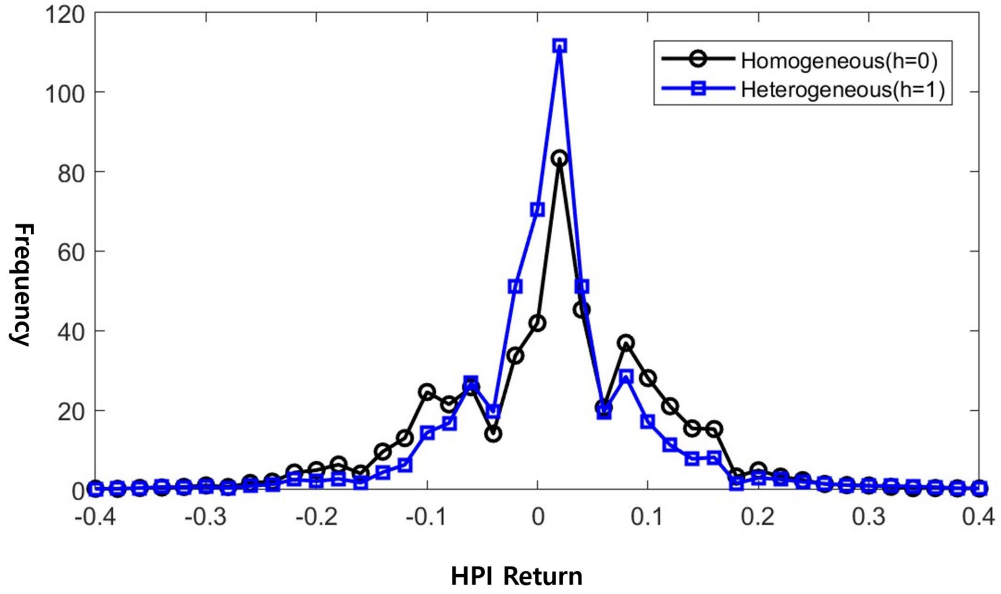

Note: This figure shows the distribution of HPI returns by heterogeneity levels in a histogram format. The horizontal axis represents the HPI return bins and the vertical axis represents the frequency. The frequency is the average value over 100 runs. The lines with circles and squares correspond to the homogeneous (h = 0) and heterogeneous (h = 1) expectation cases, respectively.

As Figure 8 shows, HPI returns follow a bell-shaped distribution. In both cases, the means appear similar, but HPI returns in the heterogeneous expectation case are clustered around the mean. The homogeneous sample appears to have a relatively thick tail. The results in Figures 12–14 imply that homogeneous expectations increase housing-market volatility. This is likely because individuals with homogeneous expectations have a greater propensity to follow trends. For instance, when the HPI is rising, buyers anticipate that house prices will continue to escalate, intensifying competition for purchases and thus maintaining an upward trend of housing prices. If this upward trend persists until prices exceed buyers' available funds, housing transactions rapidly decline. As the number of transactions decreases, singular transactions may alter the trend of HPI changes. This momentary fluctuation results in a new feedback loop. This time, a downward trend in the HPI is observed. A decrease in the HPI can result in pessimistic outlooks from agents, leading to lower prices and a sustained decline in the market. If the downward trend continues, causing housing prices to fall below the seller's reserve price, a significant drop in housing transactions will occur. The reduction in volume raises the probability of a reversal in the trend, triggering a renewed uptrend and thereby perpetuating the cycle.

The instability of the HPI is due to homogeneous expectations through this mechanism. Nevertheless, at a particular point in the preceding mechanism, when agents' expectations become heterogeneous, people's expectations are reversed. This phenomenon leads to an earlier trend reversal than that in the case of homogeneous expectations, resulting in decreased volatility. This theory suggests that as heterogeneity decreases, the housing market experiences greater volatility, and trend reversal occurs later. To verify this, we assess the standard deviation of HPI returns by heterogeneity level as in Figure 15.

Figure 15. Standard Deviation of HPI Returns by Heterogeneity

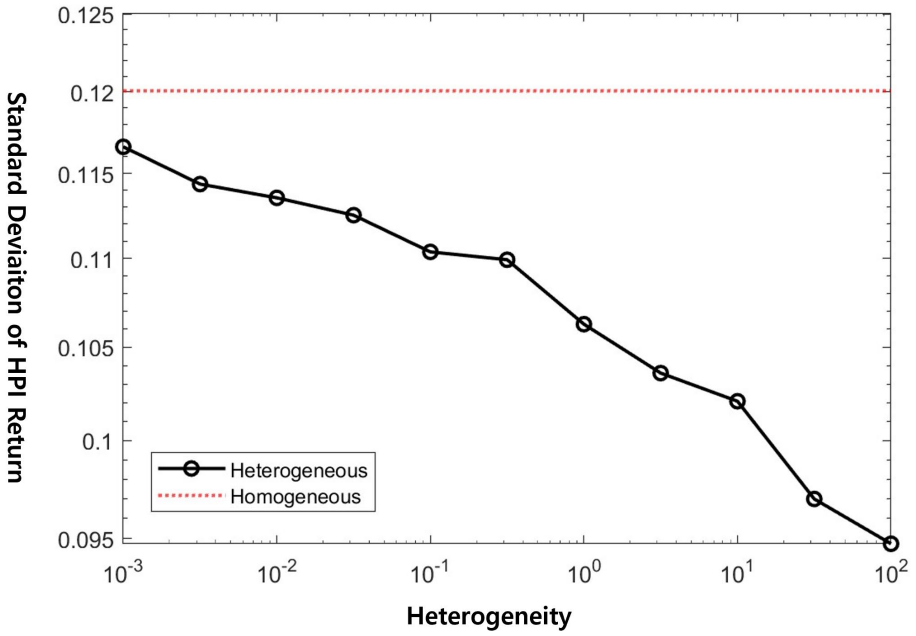

Note: This figure displays the correlation between the heterogeneity level and standard deviation of HPI returns. The horizontal axis represents the log-scaled heterogeneity level. The vertical axis denotes the standard deviation of HPI returns. The dotted horizontal line indicates the standard deviation of HPI returns when agents' expectations are homogeneous ($h = 0$). The line with circular markers represents the standard deviation of HPI returns by heterogeneity. Standard deviation values are averaged over 100 runs.

As shown in Figure 15, the standard deviation in the homogeneous expectation case exhibits the highest value. The lower the heterogeneity level, the closer the standard deviation of HPI returns to that of the homogeneous expectation case. A linear correlation exists between the log-scaled level of heterogeneity and standard deviation of HPI returns. This phenomenon, known as the "power law," is a common occurrence in complex systems. According to our model, a decrease in heterogeneity leads to a faster increase in the standard deviation of HPI returns. We can also infer that the standard deviation increases rapidly with an increase in homogeneity. This implies that agents' similar expectations strengthen feedback within the system, leading to greater volatility and intricate dynamics. Therefore, our previously proposed mechanism is likely to operate in our model.

5. Conclusion

This study examines how limited information on the value of location drives housing-price cycles. We develop an ABM for the housing market by adding houses into the Sugarscape model. Our model reflects agents' consideration of spatial components when determining housing prices. We examine how agents' vision and heterogeneous expectations influence housing prices and discover that as agents' vision widens, housing demand becomes more competitive, causing average prices and volatility to increase. In addition, when people have more homogeneous expectations, the housing market becomes more volatile.

This study expands the Sugarscape model to analyze the housing market by incorporating houses. It introduces a new direction for analyzing the housing market and successfully generates housing-price cycles by considering individuals' limited spatial information. Our results highlight the need to examine restricted spatial information as a potential cause of housing-price cycles. Additionally, we investigate the impact of heterogeneity in agents' expectations on housing price volatility, thereby providing valuable insights for policymakers, market participants, and researchers seeking a better understanding of housing market dynamics.

References

Abraham, J. M., and Hendershott, P. H. (1996). Bubbles in metropolitan housing markets. *Journal of Housing Research*, *7*(2), 191–207.

Axtell, R., Axelrod, R., Epstein, J. M., and Cohen, M. D. (1996). Aligning simulation models: A case study and results. *Computational and Mathematical Organization Theory*, *1*(2), 123–141. https://doi.org/10.1007/BF01299065

Beynier, A., Maudet, N., Rey, S., and Shams, P. (2021). Swap dynamics in single-peaked housing markets. *Autonomous Agents and Multi-Agent Systems*, *35*(2), 20. https://doi.org/10.1007/s10458-021-09503-z

Black, A., Fraser, P., and Hoesli, M. (2006). House prices, fundamentals and bubbles. *Journal of Business Finance and Accounting*, *33*(9–10), 1535–1555. https://doi.org/10.1111/j.1468-5957.2006.00638.x

Bolt, W., Demertzis, M., Diks, C., Hommes, C., and van der Leij, M. (2019). Identifying booms and busts in house prices under heterogeneous expectations. *Journal of Economic Dynamics and Control*, *103*, 234–259. https://doi.org/10.1016/j.jedc.2019.04.003

Brock, W. A., and Hommes, C. H. (1997). A rational route to randomness. *Econometrica*, *65*(5), 1059–1095. https://doi.org/10.2307/2171879

Burnside, C., Eichenbaum, M., and Rebelo, S. (2016). Understanding booms and busts in housing markets. *Journal of Political Economy*, *124*(4), 1088–1147. https://doi.org/10.1086/686732

Capozza, D. R., and Seguin, P. J. (1996). Expectations, efficiency, and euphoria in the housing market. *Regional Science and Urban Economics*, *26*(3), 369–386. https://doi.org/10.1016/0166-0462(95)02120-5

Case, K. E., and Shiller, R. J. (1989). The efficiency of the market for single-family homes. *American Economic Review*, *79*(1), 125–137.

Cheng, I.-H., Raina, S., and Xiong, W. (2014). Wall street and the housing bubble. *American Economic Review*, *104*(9), 2797–2829. https://doi.org/10.1257/aer.104.9.2797

Chinco, A., and Mayer, C. (2016). Misinformed speculators and mispricing in the housing market. *Review of Financial Studies*, *29*(2), 486–522. https://doi.org/10.1093/rfs/hhv061

Clayton, J. (1996). Rational expectations, market fundamentals and housing price volatility. *Real Estate Economics*, *24*(4), 441–470. https://doi.org/10.1111/1540-6229.00699

Clayton, J. (1997). Are housing price cycles driven by irrational expectations? *Journal of Real Estate Finance and Economics*, *14*(3), 341–363. https://doi.org/10.1023/A:1007766714810

Damianov, D. S., and Escobari, D. (2016). Long-run equilibrium shift and short-run dynamics of U.S. home price tiers during the housing bubble. *Journal of Real Estate Finance and Economics*, *53*(1), 1–28. https://doi.org/10.1007/s11146-015-9523-2

Dieci, R., and Westerhoff, F. (2012). A simple model of a speculative housing market. *Journal of Evolutionary Economics*, *22*(2), 303–329. https://doi.org/10.1007/s00191-011-0259-8

Dieci, R., and Westerhoff, F. (2016). Heterogeneous expectations, boom-bust housing cycles, and supply conditions: A nonlinear economic dynamics approach. *Journal of Economic Dynamics and Control*, *71*, 21–44. https://doi.org/10.1016/j.jedc.2016.07.011

Duca, J. V., Muellbauer, J., and Murphy, A. (2021). What drives house price cycles? International experience and policy issues. *Journal of Economic Literature*, *59*(3), 773–864. https://doi.org/10.1257/jel.20201325

Duranton, G., and Puga, D. (2004). Micro-foundations of urban agglomeration economies. *Handbook of Regional and Urban Economics*, 4(Chapter 48), 2063-2117. https://doi.org/10.1016/S1574-0080(04)80005-1

Epstein, J. M., and Axtell, R. (1996). *Growing Artificial Societies: Social Science from the Bottom Up*. Brookings Institution Press.

Erlingsson, E. J., Teglio, A., Cincotti, S., Stefansson, H., Sturluson, J. T., and Raberto, M. (2014). Housing market bubbles and business cycles in an agent-based credit economy. *Economics*, *8*(1). 20140008. https://doi.org/10.5018/economics-ejournal.ja.2014-8

Evans, B. P., Glavatskiy, K., Harré, M. S., and Prokopenko, M. (2023). The impact of social influence in Australian real estate: Market forecasting with a spatial agent-based model. *Journal of Economic Interaction and Coordination*, *18*(1), 5–57. https://doi.org/10.1007/s11403-021-00324-7

Geanakoplos, J., Axtell, R., Farmer, D. J., Howitt, P., Conlee, B., Goldstein, J., Hendrey, M., Palmer, N. M., and Yang, C.-Y. (2012). Getting at systemic risk via an agent-based model of the housing market. *American Economic Review*, *102*(3), 53–58. https://doi.org/10.1257/aer.102.3.53

Gelain, P., and Lansing, K. J. (2014). House prices, expectations, and time-varying fundamentals. *Journal of Empirical Finance*, *29*, 3–25. https://doi.org/10.1016/j.jempfin.2014.05.002

Glaeser, E. L., and Nathanson, C. G. (2017). An extrapolative model of house price dynamics. *Journal of Financial Economics*, *126*(1), 147–170. https://doi.org/10.1016/j.jfineco.2017.06.012

Glindro, E. T., Subhanij, T., Szeto, J., and Zhu, H. (2011). Determinants of house prices in nine Asia-Pacific economies. *International Journal of Central Banking*, *7*(3), 163–204.

Gomez-Gonzalez, J. E., Gamboa-Arbeláez, J., Hirs-Garzón, J., and Pinchao-Rosero, A. (2018). When bubble meets bubble: Contagion in OECD countries. *Journal of Real Estate Finance and Economics*, *56*(4), 546–566. https://doi.org/10.1007/s11146-017-9605-4

Granziera, E., and Kozicki, S. (2015). House price dynamics: Fundamentals and expectations. *Journal of Economic Dynamics and Control*, *60*, 152–165. https://doi.org/10.1016/j.jedc.2015.09.003

Hong, J., and Ryu, D. (2023). Expectations and the housing market: A model of house price dynamics. *Bulletin of Economic Research*, *forthcoming*.

Iacoviello, M. (2005). House prices, borrowing constraints, and monetary policy in the business cycle. *American Economic Review*, *95*(3), 739–764.

Iacoviello, M., and Neri, S. (2010). Housing market spillovers: Evidence from an estimated DSGE model. *American Economic Journal: Macroeconomics*, *2*(2), 125–164. https://doi.org/10.1257/mac.2.2.125

Kiyotaki, N., and Moore, J. (1997). Credit cycles. *Journal of Political Economy*, *105*(2), 211–248. https://doi.org/10.1086/262072

Laliotis, D., Buesa, A., Leber, M., and Población, J. (2020). An agent-based model for the assessment of LTV caps. *Quantitative Finance*, *20*(10), 1721–1748. https://doi.org/10.1080/14697688.2020.1733058

Lambertini, L., Mendicino, C., and Punzi, M. T. (2017). Expectations-driven cycles in the housing market. *Economic Modelling*, *60*, 297–312. https://doi.org/10.1016/j.econmod.2016.10.004

Li, J. and Wilensky, U. (2009a). *NetLogo Sugarscape 1 Immediate Growback model*. http://ccl.northwestern.edu/netlogo/models/Sugarscape1ImmediateGrowback. Center for Connected Learning and Computer-Based Modeling, Northwestern University, Evanston, IL.

Li, J. and Wilensky, U. (2009b). *NetLogo Sugarscape 2 Constant Growback model*. http://ccl.northwestern.edu/netlogo/models/Sugarscape2ConstantGrowback. Center for Connected Learning and Computer-Based Modeling, Northwestern University, Evanston, IL.

Li, J. and Wilensky, U. (2009c). *NetLogo Sugarscape 3 Wealth Distribution model*. http://ccl.northwestern.edu/netlogo/models/Sugarscape3WealthDistribution. Center for

Connected Learning and Computer-Based Modeling, Northwestern University, Evanston, IL.

McDonald, J. F., and Stokes, H. H. (2013). Monetary policy and the housing bubble. *Journal of Real Estate Finance and Economics*, *46*(3), 437–451. https://doi.org/10.1007/s11146-011-9329-9

Park, D., and Ryu, D. (2021). A machine learning-based early warning system for the housing and stock markets. *IEEE Access*, *9*, 85566–85572. https://doi.org/10.1109/ACCESS.2021.3077962

Park, D., and Ryu, D. (2022). Supply chain ethics and transparency: An agent-based model approach with *Q* -learning agents. *Managerial and Decision Economics*, *43*(8), 3331–3337. https://doi.org/10.1002/mde.3597

Park, D., and Ryu, D. (2023). Searching for and evaluating outsourced chief investment officers. *Managerial and Decision Economics*, *44*(7), 3923–3931. https://doi.org/10.1002/mde.3917

Piazzesi, M., and Schneider, M. (2009). Momentum traders in the housing market: Survey evidence and a search model. *American Economic Review*, *99*(2), 406–411. https://doi.org/10.1257/aer.99.2.406

Rahmandad, H., and Sterman, J. (2008). Heterogeneity and network structure in the dynamics of diffusion: Comparing agent-based and differential equation models. *Management Science*, *54*(5), 998–1014. https://doi.org/10.1287/mnsc.1070.0787

Shiller, R. J. (2020). *Narrative Economics: How Stories Go Viral and Drive Major Economic Events*. Princeton University Press.

Wilensky, U. (1999). *NetLogo*. http://ccl.northwestern.edu/netlogo/. Center for Connected Learning and Computer-Based Modeling, Northwestern University, Evanston, IL.

Yu, J., and Ryu, D. (2020). Effects of commodity exchange-traded note introductions: Adjustment for seasonality. *Borsa Istanbul Review*, *20*(3), 244–256. https://doi.org/10.1016/j.bir.2020.04.001